Metabolic Engineering 38 (2016) 159–169

Contents lists available at ScienceDirect

Metabolic Engineering

journal homepage: www.elsevier.com/locate/ymben

Original Research Article

Transient production of artemisinin in *Nicotiana benthamiana* is boosted by a specific lipid transfer protein from *A. annua*

Bo Wang [a,1], Arman Beyraghdar Kashkooli [a,1], Adrienne Sallets [b], Hieng-Ming Ting [a,2], Norbert C.A. de Ruijter [c], Linda Olofsson [d], Peter Brodelius [d], Mathieu Pottier [b], Marc Boutry [b], Harro Bouwmeester [a], Alexander R. van der Krol [a,*]

[a] Laboratory of Plant Physiology, Wageningen University, Droevendaalsesteeg 1, 6708 PB Wageningen, The Netherlands
[b] Institut des Sciences de la Vie, Université catholique de Louvain, Croix du Sud, 4–5, Box L7.07.14, 1348 Louvain-la-Neuve, Belgium
[c] Laboratory of Cell Biology, Wageningen University, Droevendaalsesteeg 1, 6708 PB Wageningen, The Netherlands
[d] Department of Chemistry and Biomedical Sciences, Linnaeus University, SE-38192 Kalmar, Sweden

ARTICLE INFO

Article history:
Received 8 March 2016
Received in revised form
12 June 2016
Accepted 12 July 2016
Available online 12 July 2016

Keywords:
Lipid transfer proteins
ABC transporters
Pleiotropic Drug Resistance protein
Artemisinin
Artemisia annua
Nicotiana benthamiana

ABSTRACT

Our lack of full understanding of transport and sequestration of the heterologous products currently limit metabolic engineering in plants for the production of high value terpenes. For instance, although all genes of the artemisinin/arteannuin B (AN/AB) biosynthesis pathway (AN-PW) from *Artemisia annua* have been identified, ectopic expression of these genes in *Nicotiana benthamiana* yielded mostly glycosylated pathway intermediates and only very little free (dihydro)artemisinic acid [(DH)AA]. Here we demonstrate that Lipid Transfer Protein 3 (AaLTP3) and the transporter Pleiotropic Drug Resistance 2 (AaPDR2) from *A. annua* enhance accumulation of (DH)AA in the apoplast of *N. benthamiana* leaves. Analysis of apoplast and cell content and apoplast exclusion assays show that AaLTP3 and AaPDR2 prevent reflux of (DH)AA from the apoplast back into the cells and enhances overall flux through the pathway. Moreover, AaLTP3 is stabilized in the presence of AN-PW activity and co-expression of AN-PW+*AaLTP3*+*AaPDR2* genes yielded AN and AB in necrotic *N. benthamiana* leaves at 13 days post-agroinfiltration. This newly discovered function of LTPs opens up new possibilities for the engineering of biosynthesis pathways of high value terpenes in heterologous expression systems.

1. Introduction

Artemisinin (AN) is a highly oxygenated sesquiterpene which is used to treat malaria. Both AN and arteannuin B (AB) are products of a branched biosynthesis pathway (AN-PW) in glandular trichomes on leaves and ovules from the plant *Artemisia annua*. After biosynthesis, the AB and AN precursors, artemisinic acid (AA) and dihydroartemisinic acid (DHAA), respectively, are transported to the subcuticular space of the trichomes, where (presumably through non-enzymatic oxidation) they are converted to AB and AN, respectively (Brown, 2010) (Fig. 1: AN pathway given with solid arrows).

All genes required for biosynthesis of DHAA and AA have been isolated (amorpha-4,11-diene synthase (ADS), CYP71AV1, artemisinic aldehyde Δ11(13) reductase (DBR2), aldehyde dehydrogenase 1 (ALDH1)) (Bouwmeester et al., 1999; Covello et al., 2007; Mercke et al., 2000; Teoh et al., 2009; Teoh et al., 2006; Zhang et al., 2008). Reconstitution of the AN-PW in *Nicotiana benthamiana* results in mainly glycosylated PW intermediates and only low levels of free (non-glycosylated) intermediates (dihydro) artemisinic alcohol ((DH)AAOH), (dihydro)artemisinic aldehyde ((DH)AAA) or (DH)AA (Ting et al., 2013) (Fig. 1: glycosylation reactions from endogenous *N. benthamiana* enzymes indicated by dashed arrows). It is assumed that glycosylated AN-PW products are in the vacuole and cannot contribute to AN or AB accumulation. Therefore, sequestering of (DH)AA to the apoplast could potentially help increase the yield of AN and AB in heterologous plant production platforms, but little is known about the factors involved in transport and sequestering of terpenes.

Terpene transport and sequestering activity could be by ATP-Binding Cassette (ABC) transporters and Lipid Transfer Proteins (LTP), both of which have been detected in terpene producing glandular trichome cells. ABC transporters are involved in the active transport of various metabolites. More particularly, within the ABC family, Pleiotropic Drug Resistance (PDR) transporters are localized to the plasma membrane and involved in the transport of hormones and specialized metabolites. For example, in *Nicotiana*

* Corresponding author.
[1] These authors contributed equally to this paper.
[2] Current address: Department of Biology, Norwegian University of Science and Technology, N-7491 Trondheim, Norway.

http://dx.doi.org/10.1016/j.ymben.2016.07.004
1096-7176/

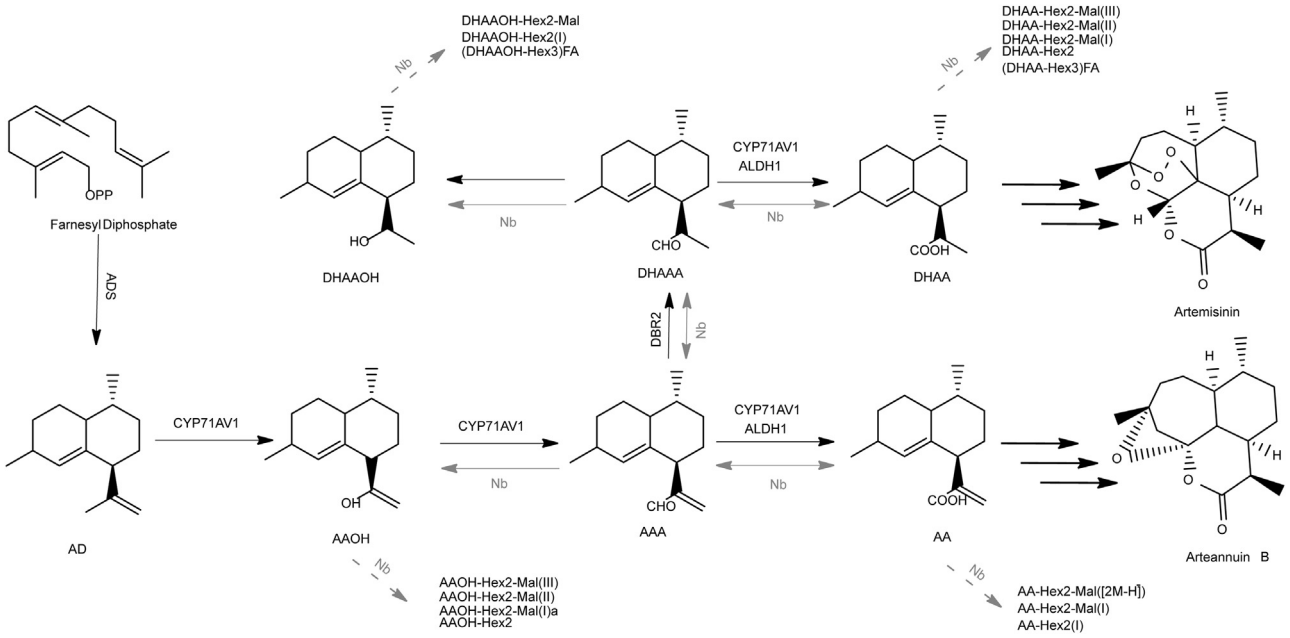

Fig. 1. Schematic representation of the artemisinin and arteannuin B biosynthetic pathway in *Artemisia annua* (Black arrows). Green arrows indicate *N. benthamiana* enzyme activities within the AN-PW, dashed green arrows indicate reactions in *N. benthamiana* draining from AN-PW. ADS, amorphadiene synthase; CYP71AV1, amorphadiene oxidase; ALDH1, aldehyde dehydrogenase; DBR2, double bond reductase. AD, Amorpha-4,11-diene; AAOH, artemisinic alcohol, AAA, artemisinic aldehyde; AA, artemisinic acid; DHAAOH, dihydroartemisinic alcohol, DHAAA, dihydroartemisinic aldehyde; DHAA, dihydroartemisinic acid. Hex, compound conjugated with hexose; Mal, compound conjugated with malonate; (I–III), different isobaric forms (i.e. identical accurate mass, but different retention times); FA, formic acid adduct.

tabacum NtPDR1 was shown to be involved in the transport of antifungal diterpenes (Crouzet et al., 2013; Stukkens et al., 2005). In the same species, a Lipid Transfer Protein (NtLTP1) was shown to be involved in diterpene secretion. Indeed diterpenes in the trichome exudate were clearly increased in the NtLTP1-over-expressing lines and decreased in the NtLTP1-RNAi lines, compared with the wild-type line (Choi et al., 2012). LTPs are small, basic proteins with a hydrophobic cavity, which are characterized in in-vitro assays by their ability to transfer lipids between membranes. Most LTP proteins contain a signal peptide sequence for secretion to the apoplast and extracellular localization of LTP proteins has been confirmed (Edstam et al., 2011; Huang et al., 2013; Kader, 1997; Yeats and Rose, 2008). Plants have multiple *LTP* genes and individual LTPs have been implicated in diverse functions like plant lipid metabolism (DeBono et al., 2009), plant defense (Salcedo et al., 2007), seed development (Edstam and Edqvist, 2014; Wang et al., 2015), sexual reproduction (Zhang et al., 2010), and cell wall extension (Nieuwland et al., 2005). However, for most LTPs the function and mode of action have not been clarified. Indications for a putative role of LTPs in terpene accumulation come from the fact that *LTP* genes show very high transcriptional activity in glandular trichomes which produce terpenes (peppermint (Lange et al., 2000), alfalfa (Aziz et al., 2005), *A. annua* (Bertea et al., 2006), hop (Wang et al., 2008), *Salvia fruticosa* (Chatzopoulou et al., 2010), tomato (Schilmiller et al., 2010) and tobacco (Harada et al., 2010)).

We identified six LTPs from *A. annua* (AaLTPs), three of which are expressed in glandular trichomes. A putative role of these AaLTPs in accumulation of AN-PW products could be tested by silencing of AaLTP expression in *A. annua* using Virus Induced Gene Silencing (VIGS). However, VIGS induced silencing was not successful in our hands. We also identified two *AaPDR* genes, which are expressed in *A. annua* trichomes. Therefore, functional analysis of the AaLTPs and AaPDRs was done using the fully reconstituted AN-PW by transient co-expression in *N. benthamiana* leaves.

2. Materials and methods

2.1. Cloning procedures

The full-length *AaLTP1*, *AaLTP2* and *AaLTP3* were amplified from cDNA made from RNA isolated from *A. annua* flowers by RACE PCR (Clontech, USA) (Bertea et al., 2006). The primer pairs AaLTP1-F/AaLTP1-R, AaLTP2-F/AaLTP2-R and AaLTP3-F/AaLTP3-R (Table S2) introduce a NcoI site at the start codon and a NotI restriction site after the stop codon of each LTP coding sequence. The PCR fragments were cloned into pIV1A2.1 vector (www.impactvector.com) between the CaMV35S promoter and the RBCS1 terminator fragment. pIV1A2.1/AaLTP1, pIV1A2.1/AaLTP2, pIV1A2.1/AaLTP3 were transferred into binary vector pBinPlus by LR reaction (Invitrogen) and the resulting pBIN/AaLTP1, pBIN/AaLTP2, and pBIN/AaLTP3 were transformed into the *A. tumefaciens* AGL-0 strain (Ting et al., 2013; van Herpen et al., 2010) which was used for the agroinfiltration experiments.

For the LTP-GFP fusion protein studies we first made an entry vector with enhanced green GFP (EGFP). The EGFP coding sequence was amplified by PCR using primers EGFP_c-term-F/EGFP_c-term-R (Table S2) by using pBinEGFP as template (http://www.wageningenur.nl/en/show/Productie-van-farmaceutische-en industriele-eiwitten-door-planten.htm). After digesting with *Not*I and *Sac*I, GFP was cloned into ImpactVectorpIV1A_2.1 (www.impactvector.com) under the control of CaMV35S promoter to generate an entry vector pIV1A_2.1/EGFP. To remove the stop codon of AaLTP1, AaLTP2 and AaLTP3, DNA fragments were amplified using the primer pairs AaLTP1_gfp-F/AaLTP1_gfp-R, AaLTP2_gfp-F/AaLTP2_gfp-R and AaLTP3_gfpF/AaLTP3_gfp-R (Table S2) by using the pIV1A_2.1/AaLTP1, pIV1A_2.1/AaLTP2 and pIV1A_2.1/AaLTP3 vectors as templates, respectively. The PCR products were digested with BamHI and NotI and subcloned into vector pIV1A_2.1/EGFP. The resulting pIV1A_2.1/AaLTP1-GFP, pIV1A_2.1/AaLTP2-GFP and pIV1A_2.1/AaLTP3-GFP containing CaMV35S promoter were cloned into the pBinPlus binary vector (Invitrogen) using LR recombination. The pBinPlus constructs containing the

35S: AaLTP1-EGFP, 35S: AaLTP2-EGFP and 35S: AaLTP3-EGFP were transferred to *A. tumefaciens* AGL-0 using electroporation.

For the LTP-RFP fusion protein genes the LTP coding sequence without stop-codon was cloned in frame to the RFP coding sequenced in TOPO vector (Invitrogen). The resulting TOPO/AaLTP1-RFP, TOPO/AaLTP2-RFP and TOPO/AaLTP3-RFP were cloned under control of CaMV35S promoter into the pK7RWG2 binary vector (http://gateway.psb.ugent.be/) using LR recombination (Invitrogen).

Partial AaPDR cDNAs were amplified from glandular trichome cDNA (Olofsson et al., 2012) using two sets of forward (AaPDR-F) and reverse (AaPDR-R) degenerated primers and cloned in pGEM-T-Easy (Promega). Full cDNAs were then obtained by RACE PCR. The PDR coding sequences were cloned between the pEn2PMA4 promoter and the tNOS terminator in the pAUX3131plasmid (De Muynck et al., 2009) and then transferred into the I-SceI site of the pPZP binary plasmid (Goderis et al., 2002). For subcellular localization, a fusion mGFP4::AaPDR2 was obtained in the pPZP vector, which already contained an mCherry gene (Mercx et al., 2016). *A. tumefaciens*-mediated transformation of *Nicotiana tabacum* BY-2 cells was performed as in Mercx et al. (2016).

2.2. Metabolite analysis

2.2.1. LC-QTOF-MS for free AN-PW products

For the AN-PW free compound analysis, the agro-infiltrated leaves were harvested, ground in liquid nitrogen. Frozen grinded samples (100 mg) were extracted in 300 μl methanol using 10 min sonication, after which the samples were centrifuged at 18,625 *g* at 4 °C. The supernatant was collected and filtered through 0.45 μm PTEE-membrane filter and diluted 10-fold with 10% methanol for analysis by a Waters Xevo tandem quadrupole mass spectrometer equipped with an electrospray ionization source and coupled to an Acquity UPLC system (Waters) as described (Ting et al., 2013). For the AN-PW glycosides and conjugations, 100 mg of infiltrated leaf material was extracted in 300 μl methanol/0.137% formic acid using 10 min sonication, after which the samples were centrifuged at 18,625*g* at 4 °C and filtered through a 0.45 μm PTEE-membrane filter. The supernatant was analyzed on a LC-QTOF-MS (Waters). Since leaves showed signs of necrosis after 7 dpi, samples collected from 7 dpi to 18 dpi were freeze-dried and yield was determined by dry-weight rather than by fresh weight. For analysis 100 mg of dried samples was used following the same extraction procedure as for fresh-weight samples.

2.3. Isolation apoplast fluid

Apoplastic fluids were collected using the infiltration centrifugation technique with modifications (Bolton et al., 2012; Witzel et al., 2011). For the vacuum infiltration, the fresh leaves were cut into 5 cm strips and stacked in a beaker filled in with deionized water. For the apoplast fluid collection, leaf strips were placed on a grid resting on the conical bottom part of 50 ml plastic centrifuge tubes (Greiner bio-one). Tubes were centrifuged at 400*g* for 15 min at 4 °C to collect the fluid in the bottom of the tubes. After collection of the released apoplast fluid the leaf strips were weighted again, and subsequently shock frozen in liquid nitrogen for the metabolites analysis. The weights were recorded before/after the infiltration and centrifugation, on average, 30–40% of the infiltrated water could be recovered by the centrifugation step.

The apoplast wash fluid was filtered through a 0.45 μm PTEE-membrane filter and the filtered fluid was dilute 5 times with 12.5% MeOH for analysis on Auity UPLC system (Waters). The concentration of the different products in the apoplast wash fluid was used to compare the different gene combinations in the transient expression assays. The transport activity in the leaf for different substrates was calculated: transport activity = mg substrate in total apoplast fluid volume ÷ mg of product in total leaf minus apoplast content.

2.4. Expression profiling in A. annua

Shoot apex and leaves from top (Leaf 1) to bottom (Leaf 10) were collected from 2-month old *A. annua* plants and pooled per leaf number for RNA extraction. From each pooled and frozen grinded sample 100 mg was extracted for gene expression analysis. RNA was isolated from the frozen grinded samples and DNase I (Invitrogen) was used to remove remaining genomic DNA. Reverse transcription was carried out with the SuperScript First-Strand Synthesis System for the cDNA synthesis (Invitrogen). Real-time quantitative PCR was performed using the iQ5 RT-PCR (BioRad). Primers used are listed in Table S2. The *A. annua* β-actin gene was used for the normalization (Lu et al., 2013; Olofsson et al., 2011). ΔΔCT was calculated as follows: ΔCT=CT(Target)-CT(Actin), ΔΔCT was normalized using ΔCT. The fold change value was calculated by $2^{-\Delta\Delta CT}$.

2.5. Transient expression in N. benthamiana leaves

The following binary expression constructs were used in pathway reconstruction experiments by transient expression in *N. benthamiana*: PW: 35S::ADS-dHMGR-FPP (A2 construct (van Herpen et al., 2010)), 35S::CYP71AV1, 35S::DBR2, 35S::ALDH1. PW*: PW+35S::HMGR. LTPs: 35S::AaLTP1, 35S::AaLTP2, 35S::AaLTP3. PDRs: 35S::AaPDR1, 35S::AaPDR2. The following binary expression constructs were used in subcellular localization studies by transient expression in *N. benthamiana*: AaLTPs and AaPDRs: 35S::AaLTP1-GFP, 35S::AaLTP2-GFP, 35S::AaLTP3-GFP.

Agroinfiltration of *N. benthamiana* leaves was done as described (van Herpen et al., 2010). The relative dosage of each *A. tumefaciens* strain between treatments within the same experiment was kept constant by dilution with *A. tumefaciens* carrying an empty vector construct. Infiltrated leaves were harvested at the days indicated (varying from 3 to 18 days post agroinfiltration). In some experiments AN-PW activity was boosted by agroinfiltration of an additional truncated HMGR expression construct (Ting et al., 2013; van Herpen et al., 2010), indicated by PW*.

2.6. Semi-quantification of LTP-EGFP fusion protein levels in agroinfiltrated leaves

Leaves expressing AaLTP-EGFP or empty vector (control) were harvested at 6 days post infiltration and four representative fully infiltrated flat regions of equal size were imaged per leaf under UV illumination at equal exposure times with a Leica MZIII fluorescence stereomicroscope. Care was taken that pixel saturation never occurred. Color images were split into individual R, G or B channels and the signal in the G channel was quantified in ImageJ 1.49 n. Four biological replicate leaves (16 individual areas) were used to determine the average fluorescence signal in the G channel for each treatment.

2.7. Subcellular localization of LTP-GFP and GFP-PDR

The LTP-GFP and GFP-PDR proteins were transiently expressed in the *N. benthamiana* leaves. Expression and targeting analysis was carried out at 5–7days post agroinfiltration (dpi) by confocal laser scanning microscopy. In order to remove air pockets from intercellular spaces in the spongy parenchyma, the leaf disks (r=0.5 cm) were mounted in perfluorodecalin (Sigma-Aldrich, P9900) (Littlejohn and Love, 2012). A Zeiss 510-META inverted confocal laser scanning microscope (Carl Zeiss, Jena, Germany)

equipped with a 63x (oil, 1.4 N. A.) Plan Apochromat DIC objective was used for image acquisition (Dong et al., 2013). Clear localizations were obtained with 1% of 488-nm Ar laser line using BP_505–530 nm for GFP and LP_560 nm to observe chlorophyll auto-fluorescence. Images were processed with Zeiss LSM image browser.

For GFP::AaPDR2, observations were performed on *N. tabacum* BY-2 cells from a five day-old culture. Cells were incubated with 10 μM FM4–64 dye for 10 min before their analysis on a LSM 710 confocal microscope (Zeiss). Excitation wavelengths were 488 nm (GFP and FM4–64) and 558 nm (mCherry). Emission wavelengths were 495–535 nm (GFP), 640–740 nm (FM4–64), and 578–620 nm (mCherry).

2.8. Apoplastic exclusion assay

Four-weeks old *N. benthamiana* leaves were infiltrated with *A. tumefaciens* harboring AaLTP3, AaPDR2, AaLTP3 + AaPDR2 or EV as the control; each together with p19. In order to achieve the highest expressed protein levels, infiltrated leaves were harvested after five days. For each treatment, four leaf disks of 1 cm diameter were excised from four individual leaves. The leaf disks were put in 6 well plate (1 leaf disc/well) and vacuum infiltrated with 3500 μl of 500 μM Na_2HPO4 buffer to make a constant flow between the buffer and apoplastic region. Then 2500 μl of solution was taken out and a solution of artemisinic acid was added into each well in a manner that each well got 0.625 mg of free compound. The 16-well plate was shaken gently for 2 h on an orbital shaker and then the leaf disks were extracted with 300 μl of MeOH and 0.1% formic acid. Extracts were analyzed by LC-QTOF-MS.

3. Results

3.1. Isolation of Artemisia annua PDR genes expressed in glandular trichomes

Analysis of the EST databases for *A. annua* identified 15 clones expressed in trichomes. In order to identify the PDR transporters highly expressed in glandular trichomes, we designed degenerated primers (Table S2) corresponding to two conserved regions of the 3′ coding sequence and surrounding a poorly conserved sequence so as to discriminate different *PDR* genes. Using these primers, cDNA clones were obtained from *A. annua* glandular trichome RNA and sequenced. Among 26 clones characterized, two genes were highly represented: AaPDR1 (NCBI EZ148819, 17 clones) and AaPDR2 (NCBI EZ144340, 8 clones).

3.2. Isolation of Artemisia annua LTP genes expressed in glandular trichomes

The six different *LTP* sequences were identified in databases resulting from *A. annua* trichome-enriched (glandular + filamentous) cDNA libraries (Bertea et al., 2006; Covello et al., 2007; Dai et al., 2010). Selection of AaLTP1–3 was based on detection of these LTP sequences in glandular trichome-enriched cDNA libraries (Ma et al., 2009; Soetaert et al., 2013) (Table S1). Subsequently three genes (AaLTP1, AaLTP2, AaLTP3) were selected for further functional analysis, based on co-expression with amorphadiene synthase gene (ADS), representing the first step in the artemisinin biosynthesis pathway, or co-expression with AaPDR1 or AaPDR2 (Fig. S1). It was noted that the expression profile in *A. annua* of AaLTP3 and AaPDR2 was distinct from that of *ADS*/*AaLTP1*/*AaLTP2*/*AaPDR1* and more closely matches the accumulation profile of (DH)AA over same leaf developmental stages (Zhang et al., 2012). The full length sequence of *AaLTP1*, *AaLTP2* and *AaLTP3* were obtained through PCR and cloned into binary expression vectors (www.impactvector.com) for subcellular localization studies and for function in the AN-PW using transient expression assays.

All three glandular-expressed *AaLTP* genes contain an N-terminal signal peptide sequence, indicative for targeting to the ER and secretion to the apoplast. We tested the subcellular targeting of AaLTP-GFP fusion proteins in transient expression assays in *N. benthamiana*. Results show that at 4 days post-agroinfiltration (dpi) the GFP signal was detected both inside and outside the cells (Fig. S2a and b), but at 7 dpi the GFP signal was mainly outside cells (Fig. S2c), which in the spongy mesophyll is visible as bridges of fluorescent material between cells. Remarkably, for all three LTP-GFP fusion proteins, the extracellular accumulation seemed to be coordinated between cells around intracellular cavities (Fig. S2c). Combined, the localization studies confirm an extracellular localization of all three AaLTPs.

3.3. AaLTPs + AaPDRs enhance freeform AN-PW products in N. benthamiana leaves

For functional analysis of the AaLTPs, the set of three *AaLTP* genes (*AaLTP1/2/3*) were co-infiltrated with the *AN-PW* genes (35S::*ADS*-tHMGR-*FPP*, 35S::*CYP71AV1*, 35S::*DBR2*, 35S::*ALDH1* (Ting et al., 2013)) and a set of two *AaPDR* genes (AaPDR1/2). In all these experiments a p19 construct was co-infiltrated to repress silencing (Voinnet et al., 2003) and relative dosage of agro-infiltrated *AN-PW* genes was kept constant by dilution with an *Agrobacterium tumefaciens* strain with empty vector (EV) where required. Free product accumulation (AAOH, AAA, AA, DHAAOH, DHAAA and DHAA) in leaves harvested at six dpi was measured by LC-trip-quad-MS (Ting et al., 2013). The co-expression of either three *AaLTPs* or two *AaPDRs* with the *AN-PW* genes has no effect on (DH)AA accumulation, and a small but significant effect on (DH)AAA and (DH)AAOH accumulation (Fig. 2). However, the combination of *AN-PW* + *AaLTPs* + *AaPDRs* results in a significant increase in accumulation of all free AN-PW products (Fig. 2), suggesting that *AaLTPs* + *AaDPRs*, can sequester these compounds away from competing sugar-conjugating or glutathione-conjugating enzyme activities in *N. benthamiana* leaves. Subsequently, we tested whether this relates to an accumulation of free AN-PW products in the apoplast of *N. benthamiana* leaves.

3.4. AN-PW products accumulate in the apoplast of N. benthamiana leaves

For analysis of product accumulation in leaf apoplast, agro-infiltrated leaves were infiltrated with water at 6 dpi and subsequently the infiltrated water was collected by mild centrifugation (Witzel et al., 2011). Analysis by UPLC-trip-quad-MS of such apoplast wash of *N. benthamiana* leaves expressing only *AN-PW* genes showed the presence of AN-PW products AAOH, AA, DHAAOH and DHAA in the apoplast (Fig. 2c). This indicates an intrinsic transport activity for these compounds in *N. benthamiana*. In contrast to total leaf extract, the intermediates (DH)AAA were not detected in the apoplast wash fluid (not shown), indicating little or no cell leakage during the apoplast wash procedure. As further control for cell leakage we measured the flavonoid rutin, which accumulates inside cells of *N. benthamiana* leaves and not in the apoplast (Markham et al., 2001; Marrs et al., 1995; Ökmen et al., 2013). No rutin was detected in apoplast fluid, indicating minimal contamination by broken cells (Fig. S3a). Analysis of apoplast samples by LC-QTOF-MS did occasionally show the presence of very low levels of DHAA-Hex3 (maximal 5% of total in whole leaf extract; Fig. S3b). Because no other glycosylated AN-PW products, which were present in the total extraction, were detected in the apoplast,

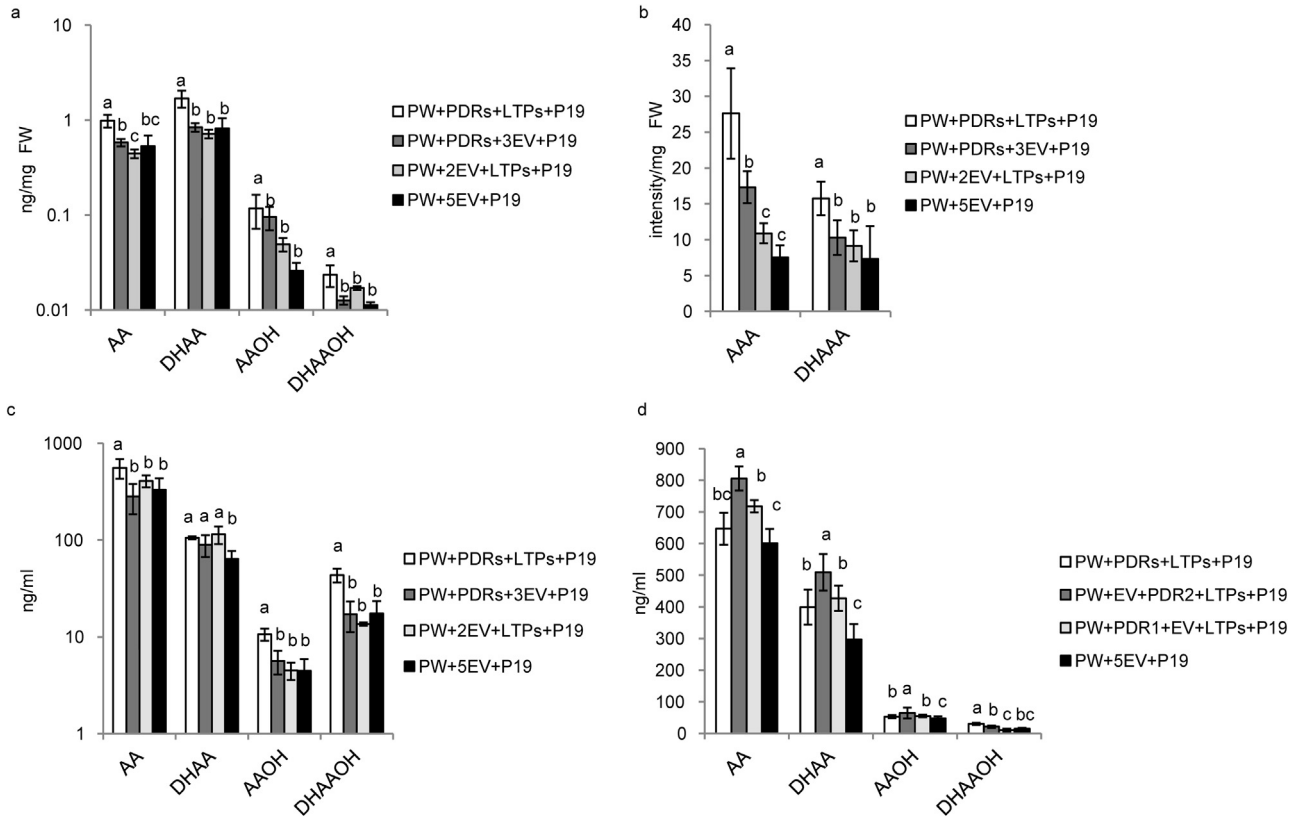

Fig. 2. Artemisinin intermediates in *N. benthamiana* infiltrated artemisinin pathway genes with the *AaLTPs* and/or *AaPDRs*. Agroinfiltrated leaves were harvested at 6 d.p.i. and leaf extracts were analyzed by LC-trip-quad-MS. (**a**) accumulation of DH(AA), DH(AAOH) in total leaf extract of *N. benthamiana* infiltrated with AN-PW or AN-PW in combinaiton with *AaLTPs* and/or *AaPDRs*. The biggest effect on free product accumulation is found for AN-PW genes coexpressed with *AaPDRs*+*AaLTPs* (2.1-fold increase for AA). (**b**) relative levels of DH(AAA) in total leaf extract (based on peak intensity because of lack of standard for (DH)AAA) of *N. benthamiana* leaves infiltrated with AN-PW or AN-PW in combinaiton with *AaLTPs* and/or *AaPDRs*. For (DH)AAA coexpression of AN-PW genes with either *PDRs* or *LTPs* both resulted in increased levels of (DH)AAA, but the effect of combined coexpression (*AaPDRs*+*AaLTPs*+AN-PW genes) was the strongest. (3.7-fold increase for AAA compared to levels in leaves infiltrated with only AN-PW genes +5xEV). (**c**) Concentration of AN-PW products in the apoplast of *N. benthamiana* infiltrated with AN-PW or AN-PW in combinaiton with *AaLTPs* and/or *AaPDRs*. Agroinfiltrated leaves were harvested at 6 d.p.i. and leaf apoplat wash was analyzed by LC-trip-quad-MS. The biggest effect on free product accumulation in the apoplast is found for AN-PW genes coexpressed with *AaPDRs*+*AaLTPs* (2.4-fold increase for AAOH, 2.5-fold increase for DHAAOH). (**d**) concentration of AN-PW products in the apoplast of *N. benthamiana* infiltrated with AN-PW or AN-PW+*AaLTPs* with *AaPDR1* or *AaPDR2*. Agroinfiltrated leaves were harvested at 6 d.p.i. and leaf apoplat wash was analyzed by LC-trip-quad-MS. The biggest increase compared to product accumulation by AN-PW genes alone was for coexpression of AN-PW genes with *AaPDR2*+*AaLTPs* (1.3-fold increase AA; 1.7-fold increase for DHAA). The relative gene dosage of AN-PW was constant between the treatments of each experiment. Statistical significant differences based on Student's *t*-test, $p < 0.05$ are indicated by letters. Error bar is SE (n=4).; In (a) & (c) scale y axis is logarithmic.

we attribute DHAA-Hex3 in the apoplast to a low intrinsic transport activity for this compound by *N. benthamiana* cells, rather than cell leakage. Analysis of apoplast wash of leaves expressing either *AN-PW*+*AaLTPs* or *AN-PW*+*AaDPRs* showed no increase in AN-PW intermediates in the apoplast, confirming results from total leaf extracts (Fig. 2c). However, expression of *AN-PW*+*AaPDRs*+*AaLTP* genes resulted in a significant increase in apoplast levels of (DH)AAOH (2.4-fold increase for AAOH, 2.5-fold increase for DHAAOH) and (DH)AA (1.7-fold increase) (Fig. 2c), again matching results from total leaf extracts. Having confirmed that the set of AaLTPs with AaPDRs enhances accumulation of AN-PW intermediates in the apoplast, we subsequently tested the specificity of the *AaLTP* gene set with either *AaPDR1* or *AaPDR2*.

3.5. AaLTPs are more effective with AaPDR2 than with AaPDR1

We tested whether there is a difference in apoplast sequestering activity for the combination *AaLTPs*+*AaPDR1*+*AN-PW* and *AaLTPs*+*AaPDR2*+*AN-PW*. Leaves agro-infiltrated with the different gene sets were harvested at 7 dpi and the apoplast fluid was isolated and analyzed by UPLC-trip-quad-MS. Results show that AaLTPs were more effective with AaPDR2 than with AaPDR1 for accumulation of (DH)AA in the apoplast (Fig. 2d). Results show that AaPDR1 and AaPDR2 have little or no effect on accumulation of (DH)AAOH, while both proteins do give an increase in (DH)AA levels in the apoplast. For apoplast accumulation of (DH)AA the AaPDR2 has a stronger activity than AaPDR1. All the PDR transporters characterized so far have been localized to the plasma membrane. Nevertheless, we checked the plasma membrane localization of AaPDRs fused to GFP and expressed in *Nicotiana tabacum* suspension cells (Fig. S4). Results show that GFP-AaPDR1 is not detected in cells expressing the fusion protein (not-shown), even though AaPDR1 is functionally active in the transient expression assays (Fig. 1d). In contrast, GFP-AaPDR2 is clearly detected in the plasma-membrane of cells where the fusion protein clearly co-localized with FM4–64, a fluorescent dye used as a plasma membrane marker (Fig. S4). Combined the results indicate a higher transport activity for AaPDR2, which in part may be explained by higher intrinsic stability of the AaPDR2 protein compared to AaPDR1.

The activity of the set of AaPDRs for (DH)AA was lower than the activity of AaPDR2 for (DH)AA alone. This could be caused by protein crowding on the plasma membrane, resulting in a competition between the active AaPDR2 and less active AaPDR1 during the high expression levels of the PDRs during transient expression. Therefore, we subsequently tested the specificity of individual *AaLTPs* in combination with the *AN-PW*+*AaPDR2*.

3.6. *AaLTP3+AaPDR2 are most active in enhancing (DH)AA levels in N. benthamiana and increasing flux through the AN-PW*

To determine whether there is a difference in activity of the individual AaLTPs, the individual *AaLTPs* were co-expressed with the *AN-PW** (PW* refers to AN-PW with additional boosting by extra HMGR: HMGR+AN-PW)+*AaDPR2* genes in *N. benthamiana* leaves. Agro-infiltrated leaves were harvested at 7 dpi and free-form AN-PW products were quantified in total leaf extracts. Since the (DH)AA are the direct precursors for the final products AN and AB, we focus on the accumulation of (DH)AA to characterize the activity of individual PDRs and LTPs. The results show that all three AaLTPs enhance the level of (DH)AA in total leaf extract, compared to only expression of *AN-PW+AaPDR2* (Fig. 3a and b). However, AaLTP3 has the biggest effect on enhancing accumulation of (DH)AA (Fig. 3a and b). Control experiment showed that the transcript levels of the individual AaLTPs in these transient assays were very similar (Fig. S5), indicating that the difference in AaLTP activity is either related to difference in individual AaLTP function and/or difference in individual LTP protein stability. Pilot studies showed that the fusion with GFP does not affect activity of the individual AaLTP proteins and therefore we used the fluorescence signal of AaLTP-GFP fusion proteins to investigate possible differences in intrinsic stability of the individual AaLTPs. Results show that GFP fluorescence of leaves expressing AaLTP3-GFP is significantly higher than that of leaves expressing AaLTP1-GFP or AaLTP2-GFP (Fig. S6), while control experiments again show that transcriptional activity of these genes is very similar. The higher accumulation of (DH)AA in the leaf in the presence of AaLTP3 therefore seems to be directly related to a higher intrinsic stability of AaLTP3. Moreover, fluorescence of AaLTP3-GFP was increased by 69% when co-expressed with *AN-PW* and *AaPDR2* genes, suggesting that AaLTP3 interacts with the AN-PW (Fig. 3c, d).

The efficiency for apoplast accumulation of individual AN-PW compounds as determined by the ratio of product level in apoplast and product level in total leaf extract, was higher for acid than for the alcohol products (Fig. 4). Not all free AN-PW products are present in the apoplast fluid, indicating that either some products are still inside the cells, or extraction of the apoplast with water is not complete. Indeed, control experiments showed that the partitioning of (DH)AA between a polar water phase and an inorganic chloroform phase is very similar to the partitioning of (DH)AA over apoplast and total leaf (Fig. S7). In contrast, the partitioning of (DH)AAOH over apoplast and total leaf is actually lower than the

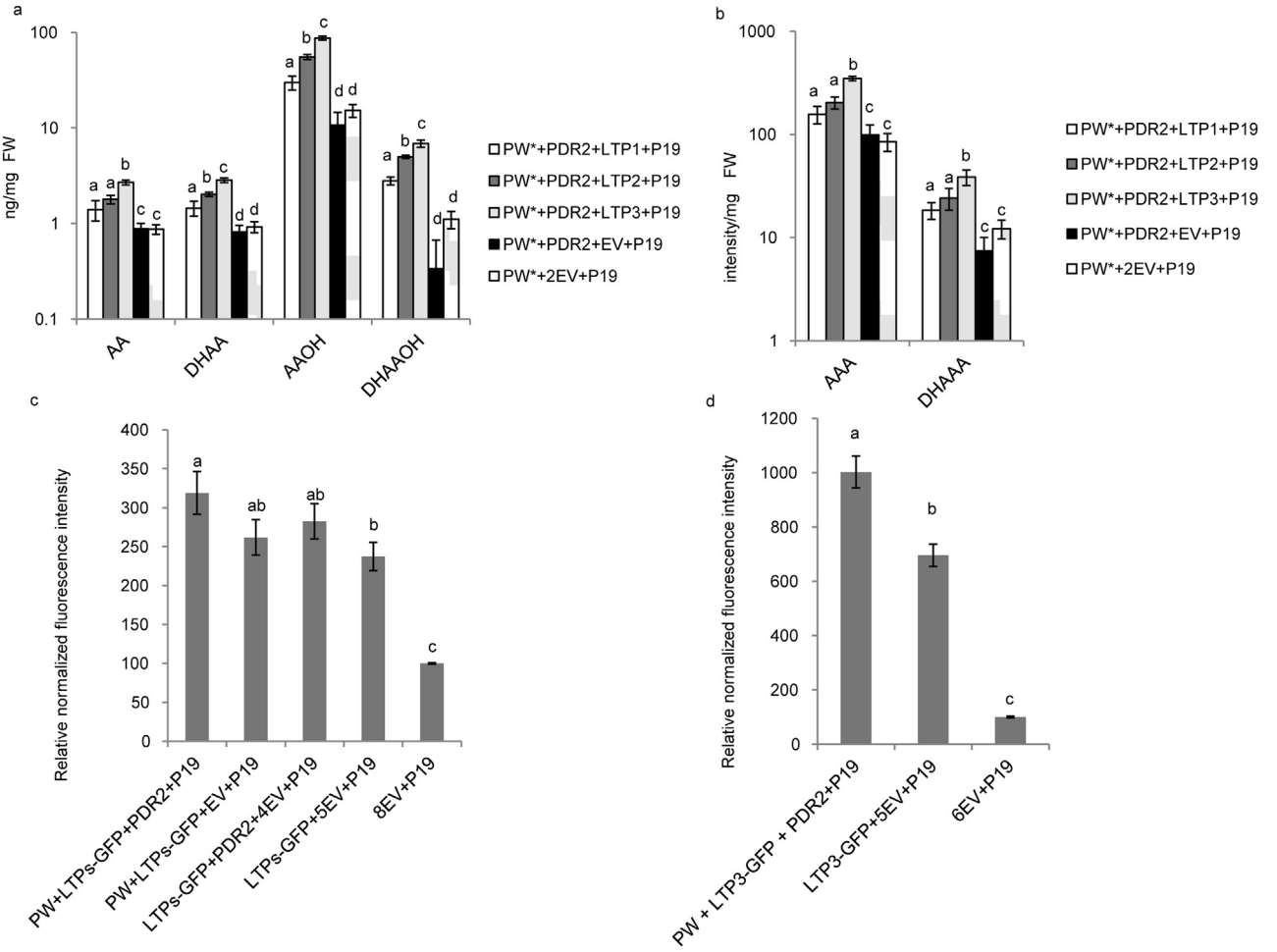

Fig. 3. AN-PW intermediates in leaf extract of *N. benthamiana* agro-infiltrated with AN-PW*+*AaPDR2* and individual *AaLTP* genes in (a) and (b). Agroinfiltrated leaves were harvested at 7 d.p.i. and leaf extract was analyzed by LC-trip-quad-MS. Error bar is SE (n=4); Note that (a) and (b) are in logarithmic scale. (**a**) accumulation of DH(AA), DH (AAOH); (**b**) relative levels of DH(AAA) (based on peak intensities due to lack standard (DH)AAA). The biggest effect of AN-PW+*PDR2* was with *AaLTP3* compared to leaves infiltrated with only AN-PW genes (+2xEV) (5.7-fold increase AAOH; 6.2-fold increase DHAAOH; 4.1-fold increase AAA). Statistical significant differences based on Student's *t*-test, $p < 0.05$ are indicated by letters. Error bar is SE; n=4. Relative fluorescence intensity of LTP-GFP transiently expressed in *N. benthamiana* increases in presence of AN PW activity in (c) and (d). (**c**) Relative fluorescence of GFP-AaLTP1+GFP-AaLTP2+AaGFP-LTP3 with or without co-expressed AN-PW+*AaPDR2* gene expression. (**d**) Relative fluorescence of LTP3-GFP with or without AN-PW+*AaDPR2* gene expression. The relative gene dosage of *LTPs-GFP* was equal between all experiments by equilibrating with EV where needed. Results of two individual experiments combined ($n \geq 54$). PW: Artemisinin Pathway constructs V5, ALDH1, P450, DBR2; PW* means AN-PW genes with an extra HMGR in the agroinfiltration; LTPs-GFP: AaLTP1-GFP+AaLTP2-GFP+AaLTP3-GFP; PDR2: AaPDR2; EV: Empty Vector.

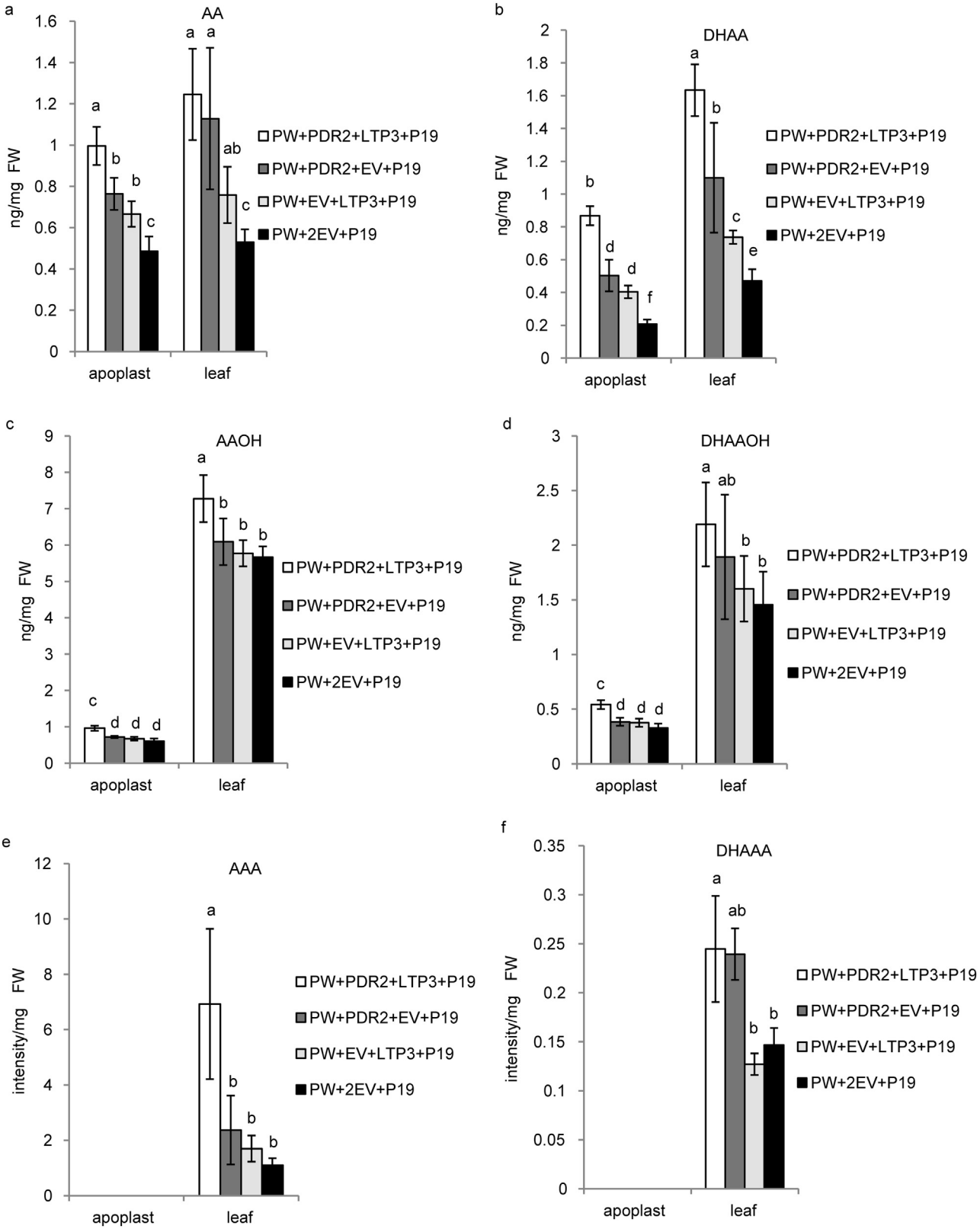

Fig. 4. AN-PW product levels in *N. benthamiana* leaf apolast and leaf cells expressing AN-PW with or without *AaLTP3* and *AaPDR2* genes. Leaves were harvested at 6 dpi. The leaf weight before and after the apoplast extraction was used to calculate the apoplast fluid not extracted from leaf. AN-PW product level remaining in leaf was calculated and corrected for product level in non-extracted apoplast fluid. The biggest effect on product accumulation in the apoplast is by coexpression of *AaPDR2*+*AaLTP3*+AN-PW genes (2.6-fold increase AA; 5.3-fold increase DHAA) compared to levels infiltrated with AN-PW+2xEV. AAOH, artemisinic alcohol; AAA, artemisinic aldehyde; AA, artemisinic acid; DHAAOH, dihydroartemisinic alcohol; DHAAA, dihydroartemisinic aldehyde; DHAA, dihydroartemisinic acid. Error bar is SE; $p < 0.05$, $n = 5$.

partitioning of (DH)AAOH between water and chloroform. We determined whether the increased accumulation of free AN-PW products by AaLTP3 has an effect on total AN-PW activity by measuring (DH)AA glycosides and glutathione conjugations by the LC-QTOF-MS in leaves expressing the different combinations of AN-PW, AaLTP3 and AaPDR2 genes. These measurements indicate that glycosylated (DH)AAOH product levels are not much affected by AaLTP3, but that glycosylated (DH)AA product levels are significantly increased by AaLTP3 (Fig. S8). This is consistent with the higher specific transport activity of AaLTP3 for (DH)AA than for (DH)AAOH. The total flux through the AN-PW is also increased by AaPDR2 and even stronger by AaLTP3+AaPDR2 (Fig. S8).

3.7. AaLTP3 blocks reflux of (DH)AA from apoplast into N. benthamiana leaf cells

Since AaLTP3 enhances AN-PW product accumulation in the apoplast when co-expressed with *AN-PW* genes, we tested whether this is due to a retention of AN-PW products by AaLTP3. Infiltration of AA or DHAA in *N. benthamiana* leaves shows very rapid uptake by cells and conversion to aldehydes and alcohols (Fig. 5a and b), which we attribute to endogenous alcohol dehydrogenase (ADH) activity. We used the uptake of AA by cells and subsequent intracellular conversion to different glycosylated products, to study the effect of AaLTP3 on retaining AA in the apoplast. Leaves expressing only EV were not able to exclude AA from the cells, resulting in high levels of AA- and DHAA-glycosides at 2 h post-substrate infiltration. Expression of only AaPDR2 was able to prevent ~27% of product conversion to glycosides, however, AaLTP3 was able to prevent ~74% of product conversion to glycosides, while the combined action of AaLTP3+AaPDR2 prevented up to ~82% of AA conversion inside the cell to glycosides (Fig. 5c). These results indicate that export of AA by AaPDR2 is not very effective when this activity is not combined with a retention system in the apoplast and that AaLTP3 functions in retention of AA in the apoplast.

3.8. AaLTP3+AaPDR2 enhance accumulation of AN and AB in N. benthamiana

The accumulation of the different pathway intermediates (AAOH, AAA, AA, DHAAOH, DHAAA, DHAA) and the desired end-products (AB and AN) in *N. benthamiana* leaves was measured at different times post-agroinfiltration (Fig. 6, S9). Results show that (DH)AA accumulates till 11 dpi, after which product levels decline again. At 7 dpi no AN or AB is detected in leaves, but these compounds start to accumulate from day 9 till 13, after which their levels start to decline. Because T-DNA from agro-infiltration may survive up to ~9 dpi (Kanagarajan et al., 2012a, 2012b), this suggests that proteins may be active till 11 dpi and that the end products AB and AN are not stable in *N. benthamiana*. In leaves expressing *AN-PW+AaPDR2+AaLTP3* we detect signs of necrosis at 9 dpi, which coincides with the first detection of AB, suggesting that necrosis may play a part in the conversion of AA to AB. Because of the leaf necrosis we did not perform apoplast measurements for samples harvested after 7 dpi.

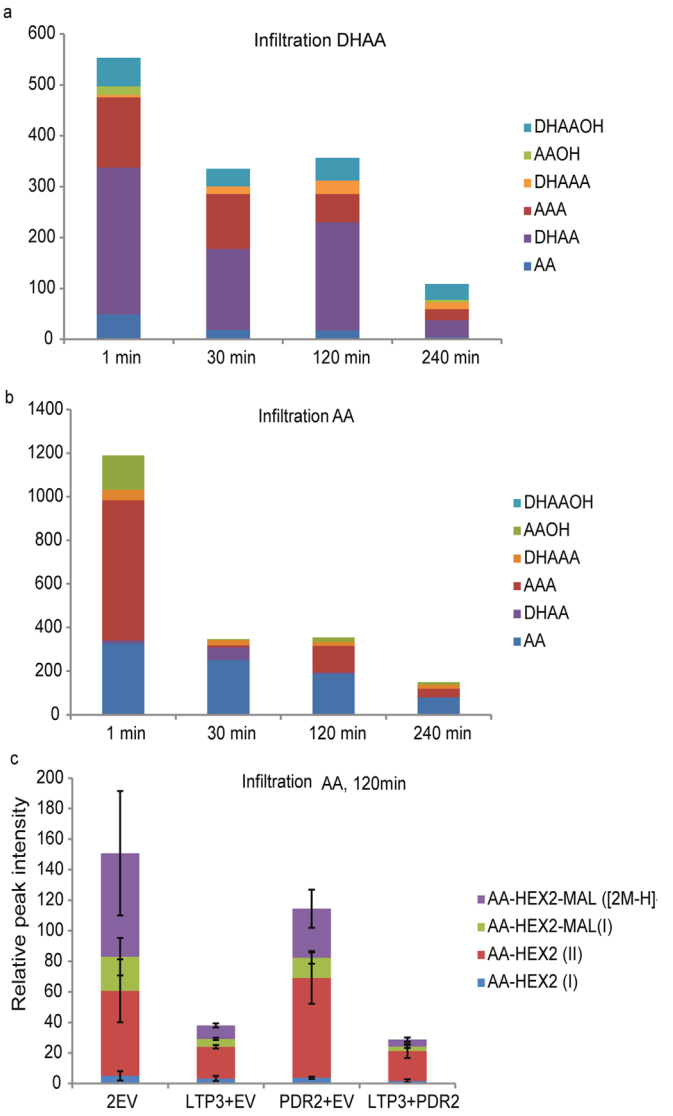

Fig. 5. Bioconversion of DHAA or AA infiltrated in *N. benthamiana* leaves. (**a**) Apoplast infiltration of DHAA (500 ng/mg) and harvest whole leaf disks at 1–240 min; (**b**) Apoplast infiltration of AA (500 ng/mg) and harvest at 0–4 h; The bioconversion of infiltrated AA or DHAA was only done once to determine the best harvest time for the exclusion experiment of Fig. 4c (no error bars). Unit of AA, DHAA, AAOH, DHAAOH is ng/mg except for AAA and DHAAA (relative peak intensity) in (a) and (b). (**c**) Semi quantification of AA entering cells after apoplast infiltration of AA (2.67 mM) at 3 dpi of *N. benthamiana* leaves expressing *AaPDR2*+EV, *AaLTP3*+EV or *AaPDR2*+*AaLTP3* at 3 dpi and harvest whole leaf disks 120 min after infiltration of AA into the apoplast. Inside the cells AA is rapidly glycosylated by addition of two hexose sugars (HEX2) which in some instances are capped by and additional malonyl group (HEX2-MAL). Different forms of AA glycosylated products elute at different times from the LC: (AA-HEX2-MAL (2 M-H), AA-HEX2-MAL (I), AA-HEX2 (I) and A-HEX2 (II). Total AA levels entering the cell are therefore quantified by combining the different peak intensities of glycosylated AA products in the chromatograms. Units are based on peak intensities of the different AA glycosylated products.

4. Discussion

4.1. AaLTP3 affects the AN biosynthesis pathway activity in N. benthamiana

Here we have investigated the role for AaLTPs and AaPDRs in AN-PW product accumulation using transient expression in *N. benthamiana*. The AaPDRs+AaLTPs together have a limited effect on boosting transport of AN-PW intermediates to the apoplast of *N. benthamiana* leaves (Fig. 2). In contrast, the effect of coexpression of only *AaPDR2+AaLTP3* with the AN-PW genes is more effective in accumulation of free AN-PW products (Fig. 3). This difference could be explained by the different number of Agrobacterium strains carrying the independent expression constructs that are used for co-infiltration into the *N. benthamiana* leaves. In Fig. 2 the total PW plus transport activity depends on co-expression of 10 genes in each cell. In Fig. 3 the total PW plus transport activity is dependent on co-transformation with 8 gene constructs.

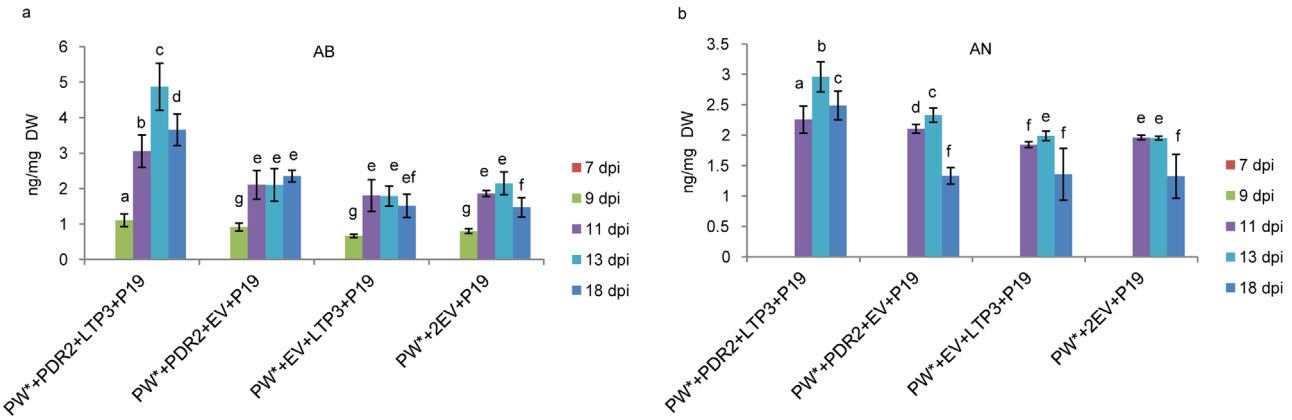

Fig. 6. Accumulation of AN and AB in leaf tissues of *N. benthamiana* agro-infiltrated with AN-PW* genes with or without *AaLTP3* and/or *AaPDR2*. Leaves were harvested at times indicated and AN and AB levels were quantified by LC-trip-quad-MS. Because around 6 dpi necrosis starts in leaves for some of the treatments, all results are expressed as ng per mg Dry Weight (DW). Error bar is SE; n=4. PW* means AN-PW genes with an extra HMGR in the agroinfiltration.

Indeed, control experiments have shown that the efficiency of co-transformation by independent agrobacterium strains that are co-infiltrated into *N. benthamiana* leaves drops off when more than 7 constructs are co-transfected. Therefore, in Fig. 2, more cells may only express (part of the) PW genes and no genes for transport activity compared to the experiment in Fig. 3.

For the two AaPDR genes we show that AaPDR2 is more effective for AN PW products (Fig. 2d). Moreover, we have collected multiple lines of evidence that AaLTP3 functions with AaPDR2 in the sequestration of AN-PW products: (1) AaLTP3 is coexpressed with AN-PW genes and PDR transporter genes in glandular trichomes (Table S1); (2) the AaLTP3 expression profile is similar to that of AaPDR2 (Fig. S1) and AaLTP3 activity on free AN-PW compound accumulation is highest in combination with AaPDR2 (Fig. 3); (3) AaLTP3 protein is extracellular (Fig. S2), while AaLTP3 enhances AN-PW product accumulation in the apoplast; (4) AaLTP3 functions in retention of AA in the apoplast (Fig. 5); (5) AaLTP3 protein stability is increased by AN-PW activity (Fig. S6) suggesting some kind of functional interaction between AaLTP3 and AN-PW activity. For production of AN/AB in the apoplast only the transport of (DH)AA supposedly would be relevant. It could be that intermediates like (DH)AAOH, which apparently are transported to the apoplast (Figs. 2c, 4c and d), recycle back into the cell for further conversion and only for the end-product (DH)AA there is a requirement to keep the product in the apoplast for conversion to AN/AB. We note that PDRs+LTPs have an effect on accumulation of (DH)AAA, a product not found in the apoplast wash. This could indicate that also inside of the cells PDRs+LTPs affect sequestering of metabolites.

4.2. The need of AaLTP3 function in planta

The experiments with apoplast infiltration of AA and DHAA have shown that both of these compounds are rapidly taken up by the cells of *N. benthamiana* and that endogenous enzyme activity in *N. benthamiana* causes a strong reverse flux of (DH)AA to (DH)AAA and (DH)AAOH. This is supposedly caused by endogenous alcohol dehydrogenases (ADHs) or oxidoreductases that reduce (DH)AA. Such activity may compromise accumulation of desired AN-PW end-products in *N. benthamiana*. A similar activity was detected in *A. annua* by Ryden et al., who characterized an oxidoreductase Red1, expressed in *A. annua* flowers that catalyses the reduction of DHAAA to DHAAOH (Rydén et al., 2010). This suggests that for heterologous expression systems and possibly also for *A. annua* the removal of (DH)AA from the cytosol through transport to and retention in the apoplast by AaLTP3 may be an important driver for the AN-PW flux towards (DH)AA. Indeed, the specific removal of (DH)AA from the endogenous AN-PW in *N. benthamiana* increased the overall flux through the AN-PW, as both free (DH)AA and glycosylated (DH)AA product accumulation were increased by co-expression of PDR2 and LTP3 (Figs. 3, 4 and S8), while there was much less effect on free and glycosylated (DH)AAOH (Fig. S8). Removal of DHAA by increased transport to the apoplast may not necessarily lower the DHAA concentration, when there is product feedback inhibition in the pathway (accumulated DHAA inhibits pathway enzyme activity). In such case, increased removal of DHAA by increased transport to the apoplast will result in similar DHAA steady state level, but with increased flux. Both the branch of transport to the apoplast and the branch towards DHAA glycosylation may benefit from the increased flux through the pathway.

4.3. Specificity of AaLTPs for AN-PW products

There are several lines of evidence that this effect of AaLTP3 is specific for (DH)AA and is not caused by generation of a general (lipid) sink for sesquiterpenes in the apoplast: (1) in contrast to AaLTP3, AaLTP1 and AaLTP2 have little or no effect on free (DH)AA accumulation in the apoplast. (2) AaLTP3 protein stability is increased by AN-PW activity. Finally, transient co-expression of AaLTP3 with the costunolide biosynthetic pathway from feverfew (a sesquiterpene PW very similar to the AN-PW; (Liu et al., 2011)) in *N. benthamiana* did not affect costunolide accumulation, suggesting specificity for (DH)AA and not any other lipid molecule.

4.4. Putative model of AaLTP3 function

The retention activity of AaLTP3 for AA cannot be explained by a simple 1:1 binding to AA. If we assume an extreme high AaLTP3 production at 3 dpi of 1 mg/g FW in *N. benthamiana*, the estimated molar ratio of (AaLTP3): (infiltrated AA) is approximately 1:635. Although at present we can only speculate on how AaLTP3 fulfills the retention activity in the apoplast, we favor the model in which AaLTP3 transports AN-PW products from the space between the plasma-membrane and the cell wall to the other side of the cell wall at the site of inter cellular spaces. Once deposited at this site a reflux back into the cell is then largely prevented. The empty LTP may subsequently diffuse back to the plasma membrane to be reloaded by another (DH)AA molecule. The characterization of the AaLTP3 and AaPDR2 has here been done in the context of *N. benthamiana* leaf cells and not in the context of secretory trichome cells. Although by agroinfiltration of *N. benthamiana* leaves leaf epidermal cells are also subject to transformation, we did not find any evidence that export of AN-PW products was enhanced in the

epidermal cell layer (e.g. rapid chloroform dipping, which is sufficient to release AN from glandular trichomes of *A. annua*, was not sufficient to extract AN-PW products from *N. benthamiana* leaves expressing AN-PW genes+*AaPDR2*+*AaLTP3*). Glandular trichomes of *A. annua* are fully specialized in producing AN/AB and part of the secretion system active in such specialized cells may still be missing in our reconstituted system of AN-PW+*PDR*+*LTP* genes. Finally, the insight that LTPs may be needed to remove secreted products from the plasma membrane to prevent reflux opens up new possibilities in the engineering of biosynthesis pathways of high value terpenes in heterologous expression systems.

Author contributions

Bo Wang and Arman Beyraghdar Kashkooli contributed to the transient assays in *N. benthamiana*, fluorescent protein stability assays, product exclusion assay and writing the manuscript. Adrienne Sallets provided data on transport function and Mathieu Pottier provided data on subcellular localization of AaPDR1 and AaPDR2. Hieng-Ming Ting cloned the AaLTP genes, Norbert C. A. de Ruijter assisted in confocal microscopy, Linda Olofsson and Peter Brodelius contributed to the cloning of the AaPDR genes and localization of PDR expression. Marc Boutry and Harro Bouwmeester contributed by improving the manuscript. Alexander R. van der Krol provided the concept of testing LTPs in terpene transport, testing PDRs in transient expression assays, testing LTPs and PDRs in product exlusion assays and helped writing the manuscript.

Acknowledgments

We thank Miriam Goedbloed, Marielle Schreuder, Joseph Nader and Jacqueline Busscher-Lange for helpful assistance in the laboratory, Bert Schipper for assistance in LC-QTOF-MS analysis, Francel Verstappen and Kristyna Flokova for help in LC-trip-quad-MS analysis. Research by Hieng Ting Ming was funded by Research School Experimental Plant Sciences The Netherlands, research by Bo Wang was funded by China Scholarship Counsel and research by Arman Beyraghdar Kashkooli was funded by the Iranian Ministry of Science Research and Technology.

Appendix A. Supporting information

Supplementary data associated with this article can be found in the online version at http://dx.doi.org/10.1016/j.ymben.2016.07.004.

References

Aziz, N., Paiva, N., May, G., Dixon, R., 2005. Transcriptome analysis of alfalfa glandular trichomes. Planta 221, 28–38.
Bertea, C.M., Voster, A., Verstappen, F.W.A., Maffei, M., Beekwilder, J., Bouwmeester, H.J., 2006. Isoprenoid biosynthesis in Artemisia annua: Cloning and heterologous expression of a germacrene A synthase from a glandular trichome cDNA library. Arch. Biochem. Biophys. 448, 3–12.
Bolton, M.D., Thomma, B.P.H.J., Joosten, M.A.J., 2012. Isolation of apoplastic fluid from leaf tissue by the vacuum iInfiltration-centrifugation technique. Plant Fungal Pathogens vol. 835. Humana Press, pp. 603–610.
Bouwmeester, H.J., Wallaart, T.E., Janssen, M.H.A., Van Loo, B., Jansen, B.J.M., Posthumus, M.A., Schmidt, C.O., De Kraker, J.-W., König, W.A., Franssen, M.C.R., 1999. Amorpha-4,11-diene synthase catalyses the first probable step in artemisinin biosynthesis. Phytochemistry 52, 843–854.
Brown, G.D., 2010. The biosynthesis of Artemisinin Qinghaosu and the phytochemistry of Artemisia annua L. (Qinghao). Molecules 15, 7603–7698.
Chatzopoulou, F., Makris, A., Argiriou, A., Degenhardt, J., Kanellis, A., 2010. EST analysis and annotation of transcripts derived from a trichome-specific cDNA library from Salvia fruticosa. Plant Cell Rep. 29, 523–534.
Choi, Y.E., Lim, S., Kim, H.-J., Han, J.Y., Lee, M.-H., Yang, Y., Kim, J.-A., Kim, Y.-S., 2012. Tobacco NtLTP1, a glandular-specific lipid transfer protein, is required for lipid secretion from glandular trichomes. Plant J. 70, 480–491.
Covello, P.S., Teoh, K.H., Polichuk, D.R., Reed, D.W., Nowak, G., 2007. Functional genomics and the biosynthesis of artemisinin. Phytochemistry 68, 1864–1871.
Crouzet, J., Roland, J., Peeters, E., Trombik, T., Ducos, E., Nader, J., Boutry, M., 2013. NtPDR1, a plasma membrane ABC transporter from Nicotiana tabacum, is involved in diterpene transport. Plant Mol. Biol. 82, 181–192.
Dai, X., Wang, G., Yang, D.S., Tang, Y., Broun, P., Marks, M.D., Sumner, L.W., Dixon, R. A., Zhao, P.X., 2010. TrichOME: a comparative omics database for plant trichomes. Plant Physiol. 152, 44–54.
De Muynck, B., Navarre, C., Nizet, Y., Stadlmann, J., Boutry, M., 2009. Different subcellular localization and glycosylation for a functional antibody expressed in Nicotiana tabacum plants and suspension cells. Transgenic Res. 18, 467–482.
DeBono, A., Yeats, T.H., Rose, J.K.C., Bird, D., Jetter, R., Kunst, L., Samuels, L., 2009. *Arabidopsis* LTPG Is a glycosylphosphatidylinositol-anchored lipid transfer protein required for export of lipids to the plant surface. Plant Cell. 21, 1230–1238.
Dong, L., Miettinen, K., Goedbloed, M., Verstappen, F.W.A., Voster, A., Jongsma, M.A., Memelink, J., Krol, S. v d, Bouwmeester, H.J., 2013. Characterization of two geraniol synthases from Valeriana officinalis and Lippia dulcis: Similar activity but difference in subcellular localization. Metab. Eng. 20, 198–211.
Edstam, M.M., Edqvist, J., 2014. Involvement of GPI-anchored lipid transfer proteins in the development of seed coats and pollen in *Arabidopsis thaliana*. Physiol. Plant. 152, 32–42.
Edstam, M.M., Viitanen, L., Salminen, T.A., Edqvist, J., 2011. Evolutionary history of the non-specific lipid transfer. Proteins Mol. Plant 4, 947–964.
Goderis, I.J.W.M., De Bolle, M.F.C., François, I.E.J.A., Wouters, P.F.J., Broekaert, W.F., Cammue, B.P.A., 2002. A set of modular plant transformation vectors allowing flexible insertion of up to six expression units. Plant Mol. Biol. 50, 17–27.
Harada, E., Kim, J.-A., Meyer, A.J., Hell, R., Clemens, S., Choi, Y.-E., 2010. Expression profiling of tobacco leaf trichomes identifies genes for biotic and abiotic stresses. Plant Cell Physiol. 51, 1627–1637.
Huang, M.-D., Chen, T.-L.L., Huang, A.H.C., 2013. Abundant type III lipid transfer proteins in arabidopsis tapetum are secreted to the locule and become a constituent of the pollen exine. Plant Physiol. 163, 1218–1229.
Kader, J.C., 1997. Lipid-transfer proteins: a puzzling family of plant proteins. Trends Plant Sci. 2, 66–70.
Kanagarajan, S., Muthusamy, S., Gliszczyńska, A., Lundgren, A., Brodelius, P.E., 2012a. Functional expression and characterization of sesquiterpene synthases from *Artemisia annua* L. using transient expression system in *Nicotiana benthamiana*. Plant Cell Rep. 31, 1309–1319.
Kanagarajan, S., Tolf, C., Lundgren, A., Waldenström, J., Brodelius, P.E., 2012b. Transient expression of hemagglutinin antigen from low pathogenic avian influenza A (H7N7) in *Nicotiana benthamiana*. PLoS One 7, e33010.
Lange, B.M., Wildung, M.R., Stauber, E.J., Sanchez, C., Pouchnik, D., Croteau, R., 2000. Probing essential oil biosynthesis and secretion by functional evaluation of expressed sequence tags from mint glandular trichomes. Proc. Natl. Acad. Sci. USA 97, 2934–2939.
Littlejohn, G.R., Love, J., 2012. A simple method for imaging arabidopsis leaves using perfluorodecalin as an infiltrative imaging medium. J. Visual. Exp. (JoVE), 3394.
Liu, Q., Majdi, M., Cankar, K., Goedbloed, M., Charnikhova, T., Verstappen, F.W.A., de Vos, R.C.H., Beekwilder, J., van der Krol, S., Bouwmeester, H.J., 2011. Reconstitution of the costunolide biosynthetic pathway in yeast and *Nicotiana benthamiana*. PLoS One 6, e23255.
Lu, X., Zhang, L., Zhang, F., Jiang, W., Shen, Q., Zhang, L., Lv, Z., Wang, G., Tang, K., 2013. AaORA, a trichome-specific AP2/ERF transcription factor of Artemisia annua, is a positive regulator in the artemisinin biosynthetic pathway and in disease resistance to Botrytis cinerea. New Phytol. 198, 1191–1202.
Ma, C., Wang, H., Lu, X., Wang, H., Xu, G., Liu, B., 2009. Terpenoid metabolic profiling analysis of transgenic Artemisia annua L. by comprehensive two-dimensional gas chromatography time-of-flight mass spectrometry. Metabolomics 5, 497–506.
Markham, K.R., Gould, K.S., Ryan, K.G., 2001. Cytoplasmic accumulation of flavonoids in flower petals and its relevance to yellow flower colouration. Phytochemistry 58, 403–413.
Marrs, K.A., Alfenito, M.R., Lloyd, A.M., Walbot, V., 1995. A glutathione S-transferase involved in vacuolar transfer encoded by the maize gene Bronze-2. Nature 375, 397–400.
Mercke, P., Bengtsson, M., Bouwmeester, H.J., Posthumus, M.A., Brodelius, P.E., 2000. Molecular cloning, expression, and characterization of Amorpha-4,11-diene synthase, a key enzyme of artemisinin biosynthesis in Artemisia annua L. Arch. Biochem. Biophys. 381, 173–180.
Mercx, S., Tollet, J., Magy, B., Navarre, C., Boutry, M., 2016. Gene inactivation by CRISPR-Cas9 in *Nicotiana tabacum* BY-2 Suspension Cells. Front. Plant Sci., 7.
Nieuwland, J., Feron, R., Huisman, B.A.H., Fasolino, A., Hilbers, C.W., Derksen, J., Mariani, C., 2005. Lipid transfer proteins enhance cell wall extension in tobacco. Plant Cell. 17, 2009–2019.
Ökmen, B., Etalo, D.W., Joosten, M.H.A.J., Bouwmeester, H.J., de Vos, R.C.H., Collemare, J., de Wit, P.J.G.M., 2013. Detoxification of α-tomatine by Cladosporium fulvum is required for full virulence on tomato. New Phytol. 198, 1203–1214.
Olofsson, L., Engström, A., Lundgren, A., Brodelius, P.E., 2011. Relative expression of genes of terpene metabolism in different tissues of *Artemisia annua* L. BMC Plant Biol. 11, 45.
Olofsson, L., Lundgren, A., Brodelius, P.E., 2012. Trichome isolation with and without fixation using laser microdissection and pressure catapulting followed by RNA amplification: Expression of genes of terpene metabolism in apical and sub-

apical trichome cells of *Artemisia annua* L. Plant Sci. 183, 9–13.
Rydén, A.-M., Ruyter-Spira, C., Quax, W.J., Osada, H., Muranaka, T., Kayser, O., Bouwmeester, H., 2010. The molecular cloning of dihydroartemisinic aldehyde reductase and its implication in artemisinin biosynthesis in Artemisia annua. Planta MEd. 76, 1778–1783.
Salcedo, G., Sánchez-Monge, R., Barber, D., Díaz-Perales, A., 2007. Plant non-specific lipid transfer proteins: an interface between plant defence and human allergy. Biochim. Biophys. Acta (BBA) - Mol. Cell Biol. Lipids 1771, 781–791.
Schilmiller, A.L., Miner, D.P., Larson, M., McDowell, E., Gang, D.R., Wilkerson, C., Last, R.L., 2010. Studies of a biochemical factory: tomato trichome deep expressed sequence tag sequencing and proteomics. Plant Physiol. 153, 1212–1223.
Soetaert, S., Van Neste, C., Vandewoestyne, M., Head, S., Goossens, A., Van Nieuwerburgh, F., Deforce, D., 2013. Differential transcriptome analysis of glandular and filamentous trichomes in Artemisia annua. BMC Plant Biol. 13, 220.
Stukkens, Y., Bultreys, A., Grec, S., Trombik, T., Vanham, D., Boutry, M., 2005. NpPDR1, a pleiotropic drug resistance-type ATP-binding cassette transporter from *Nicotiana plumbaginifolia*, plays a major role in plant pathogen defense. Plant Physiol. 139, 341–352.
Teoh, K.H., Polichuk, D.R., Reed, D.W., Covello, P.S., 2009. Molecular cloning of an aldehyde dehydrogenase implicated in artemisinin biosynthesis in *Artemisia annua*. Botany 87, 635–642.
Teoh, K.H., Polichuk, D.R., Reed, D.W., Nowak, G., Covello, P.S., 2006. Artemisia annua L. (Asteraceae) trichome-specific cDNAs reveal CYP71AV1, a cytochrome P450 with a key role in the biosynthesis of the antimalarial sesquiterpene lactone artemisinin. FEBS Lett. 580, 1411–1416.
Ting, H.-M., Wang, B., Rydén, A.-M., Woittiez, L., van Herpen, T., Verstappen, F.W.A., Ruyter-Spira, C., Beekwilder, J., Bouwmeester, H.J., van der Krol, A., 2013. The metabolite chemotype of Nicotiana benthamiana transiently expressing artemisinin biosynthetic pathway genes is a function of CYP71AV1 type and relative gene dosage. New Phytol. 199, 352–366.
van Herpen, T.W., Cankar, K., Nogueira, M., Bosch, D., Bouwmeester, H.J., Beekwilder, J., 2010. *Nicotiana benthamiana* as a production platform for artemisinin precursors. PLoS One 5, e14222.
Voinnet, O., Rivas, S., Mestre, P., Baulcombe, D., 2003. An enhanced transient expression system in plants based on suppression of gene silencing by the p19 protein of tomato bushy stunt virus. Plant J. 33, 949–956.
Wang, G., Tian, L., Aziz, N., Broun, P., Dai, X., He, J., King, A., Zhao, P.X., Dixon, R.A., 2008. Terpene biosynthesis in glandular trichomes of hop. Plant Physiol. 148, 1254–1266.
Wang, X., Zhou, W., Lu, Z., Ouyang, Y., C. S, O., Yao, J., 2015. A lipid transfer protein, OsLTPL36, is essential for seed development and seed quality in rice. Plant Sci. 239, 200–208.
Witzel, K., Shahzad, M., Matros, A., Mock, H.-P., Muhling, K., 2011. Comparative evaluation of extraction methods for apoplastic proteins from maize leaves. Plant Methods 7, 48.
Yeats, T.H., Rose, J.K.C., 2008. The biochemistry and biology of extracellular plant lipid-transfer proteins (LTPs). Protein Sci. 17, 191–198.
Zhang, D., Liang, W., Yin, C., Zong, J., Gu, F., Zhang, D., 2010. OsC6, encoding a lipid transfer protein, is required for postmeiotic anther development in rice. Plant Physiol. 154, 149–162.
Zhang, L., Lu, X., Shen, Q., Chen, Y., Wang, T., Zhang, F., Wu, S., Jiang, W., Liu, P., Zhang, L., Wang, Y., Tang, K., 2012. Identification of putative Artemisia annua ABCG transporter unigenes related to Artemisinin yield following expression analysis in different plant tissues and in response to methyl Jasmonate and Abscisic acid treatments. Plant Mol. Biol. Rep. 30, 838–847.
Zhang, Y., Teoh, K.H., Reed, D.W., Maes, L., Goossens, A., Olson, D.J.H., Ross, A.R.S., Covello, P.S., 2008. The molecular cloning of artemisinic aldehyde Δ11(13) reductase and its role in glandular trichome-dependent biosynthesis of artemisinin in Artemisia annua. J. Biol. Chem. 283, 21501–21508.